Generation of terahertz radiation under the effect of a femtosecond pulse on plasma in a magnetic field

K. N. Ovchinnikov and S. A. Uryupin*

Lebedev Physical Institute, Russian Academy of Sciences, Leninsky prospect 53, Moscow 119991, Russia

The generation of terahertz (THz) radiation under the effect of a femtosecond laser pulse on a transparent semibounded plasma in a constant magnetic field is studied. It is shown how the generation patterns of THz radiation depend on the laser pulse duration and the ratio between the cyclotron and plasma frequencies of electrons. In each of the modes considered, the total energy per unit area, spectral composition, and pulse shape of the generated THz radiation are found. It has been established that optimal generation conditions are realized at laser pulse duration comparable to the reciprocal frequency of plasma oscillations and at electron cyclotron frequency lower than plasma frequency. When cyclotron frequency exceeds plasma frequency, the possibility of increasing the generation frequency up to frequencies comparable to the cyclotron frequency is revealed.

I. INTRODUCTION

The influence of constant magnetic field on the generation of terahertz (THz) radiation in plasma has been studied for a relatively long time. Interest in such studies is due to the emergence of additional possibilities to control the intensity, spectral composition, and pulse shape of the generated radiation. The effect of magnetic field on the generation of THz radiation by a wake wave propagating across magnetic field was studied in [1–3]. In [4], the generation of THz radiation was studied under the conditions when the wake wave propagates along the magnetic field. Considerable attention was paid to the study of THz radiation generation by mixing two laser beams in magnetoactive plasma (see [5–9]), including those with periodically modulated electron density [10–13]. The THz radiation produced by the effect of a femtosecond laser pulse on dense plasma occupying a half-space in constant magnetic field directed along the plasma boundary was studied in [14,15]. The generation arose under the effect of ponderomotive force localized in the skin layer and changing during the pulse duration. In contrast to [14,15], where the equations for the average electron velocity were used to describe the effect of a femtosecond pulse on electrons, in [16] the kinetic equation for electrons was used to study the generation of THz radiation in magnetoactive plasma. In this case, in [16] the laser radiation frequency was considered to be higher than the electron plasma frequency. In [16] the main attention was paid to the description of the THz radiation generation in strong magnetic field, when the electron Larmor radius is less than both the characteristic spatial scale of the laser pulse and the ratio of the light speed to the electron plasma frequency and the generation frequency is less than the electron cyclotron frequency. Due to the use of the above restrictions on the value of the electron cyclotron frequency,

a fairly complete description of the features of generation in [16] turned out to be possible in a strong magnetic field, when cyclotron frequency Ω is greater than plasma frequency ω_L and the laser pulse duration is greater than ω_L^2/Ω.

This paper is devoted to the description of generation under conditions not considered in [16], as well as to a more detailed analysis of the pulse shape and spectral composition of the generated radiation. Below, the equation for a low-frequency magnetic field in plasma is obtained by using the expression for the low-frequency current arising under the effect of low-frequency field and ponderomotive force. Using the continuity conditions for the tangential components of the electric and magnetic fields, after matching solutions of this equation and its analog in vacuum, the low-frequency field is found at the plasma boundary. The total energy per unit area, low-frequency magnetic field, and spectral energy density of the THz radiation are studied in the cases of weak and strong constant magnetic field. When the electron cyclotron frequency is higher than the plasma frequency, three different modes are considered that correspond to different laser pulse durations. It is shown that when exposed to a long laser pulse, radiation is generated at frequencies comparable to the reciprocal of the pulse duration, and the low-frequency pulse shape is described by the second derivative of the laser pulse intensity envelope. When exposed to a laser pulse of intermediate duration, the spectral energy density of low-frequency radiation has a peak at the frequency of the order of the ratio of the plasma frequency squared to the cyclotron frequency and a wide plateau in the frequency range below the reciprocal pulse duration. In this case, the generated pulse has a sharp peak, the duration of which is the same as that of the laser pulse, and contains oscillations with the frequency of the extraordinary wave. If the plasma is affected by a short laser pulse, then the generation peak occurs at frequencies comparable to the electron cyclotron frequency. Herein the generated pulse contains oscillations at a frequency close to the cyclotron one, and the pulse envelope contains beats at a lower frequency. In
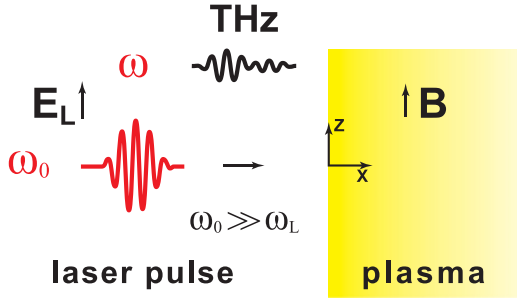
*uryupin@sci.lebedev.ru

FIG. 1. Schematic of THz generation under the effect of a femtosecond laser pulse on a transparent semibounded plasma in a constant magnetic field.

a relatively weak magnetic field, when the electron cyclotron frequency is less than the plasma frequency, two modes are possible. If the laser pulse duration is longer than the period of plasma oscillations, then generation patterns of low-frequency radiation are similar to those that occur when a long pulse acts on plasma in strong magnetic field. If the laser pulse duration is less than the period of the plasma oscillations, then radiation with frequencies close to the electron plasma frequency is mainly generated. The low-frequency radiation pulse contains oscillations at the plasma frequency and weakly pronounced beats at a lower frequency. It has been established that the optimal generation conditions are realized at a laser pulse duration comparable to the period of plasma oscillations and under the condition that the cyclotron frequency of electrons does not exceed the plasma one.

II. LOW-FREQUENCY FIELD IN PLASMA

Let us consider a plasma in static magnetic field $\mathbf{B} = (0, 0, B)$ occupying the region $x > 0$ (see Fig. 1). For example, it can be a plasma with direct discharge along a constant magnetic field. The density of such a plasma varies over a wide range from 10^{15} to 10^{19} cm^{-3}, and plasma temperature is several eV and higher. Due to the presence of a constant magnetic field, the plasma confinement time is much longer than the THz pulse generation time. We assume that plasma interacts with the laser pulse, whose electric field has the form $(1/2)\mathbf{E}_L \exp(-i\omega_0\tau - \tau^2/2t_p^2) + $ c.c., where $\mathbf{E}_L = (0, 0, E_L)$, ω_0 is the carrier frequency of the laser radiation, $\omega_0 t_p \gg 1$, $\tau = t - x/c$, and c is the speed of light. The value of t_p determines the pulse width at half height $\tau_p = 2t_p\sqrt{\ln 2}$. The frequency ω_0 is assumed to be much greater than the plasma electron frequency ω_L: $\omega_0 \gg \omega_L$. Here $\omega_L = \sqrt{4\pi n e^2/m}$, n is the electron density, and e and m are the electron charge and mass, respectively. When such a high-frequency field affects the plasma, the corrections due to the frequency and spatial dispersion are small, and the field strength in the plasma is approximately described by the same expression as in vacuum. The high-frequency field with a slowly changing envelope produces a ponderomotive potential of the form $\Phi = (e^2|\mathbf{E}_L|^2/4m\omega_0^2)\exp(-\tau^2/t_p^2)$. Due to the inhomogeneity of the ponderomotive potential along the axis ox, a ponderomotive force arises. This force leads to the low-frequency motions of electrons. As a result

currents and fields with frequencies $\omega \ll \omega_0$ are generated in the plasma. If thermal motion of electrons is unimportant, then Fourier images of the low-frequency current density $\mathbf{j}(x, \omega) = (j_x(x, \omega), j_y(x, \omega, 0))$ and field $\mathbf{E}(x, \omega) = (E_x(x, \omega), E_y(x, \omega), 0)$ are related by the equation [14,15]

$$j_\alpha(x, \omega) = \sigma_{\alpha\beta}(\omega)\left[\mathbf{E}(x, \omega) - \frac{1}{e}\nabla\Phi(x, \omega)\right]_\beta, \quad (1)$$

where $\sigma_{\alpha\beta}(\omega)$ is the electrical conductivity tensor

$$\sigma_{\alpha\beta}(\omega) = \frac{1}{4\pi}\frac{\omega_L^2}{\omega^2 - \Omega^2}(i\omega\delta_{\alpha\beta} + \Omega\epsilon_{\alpha\beta s}b_s), \quad (2)$$

$\Omega = |eB/mc|$ is the electron cyclotron frequency, $\delta_{\alpha\beta}$ is the Kronecker delta symbol, $\epsilon_{\alpha\beta s}$ is the third rank Levi-Civita symbol, $\mathbf{b} = \mathbf{B}/B = (0, 0, 1)$ is the unit vector along the constant magnetic field, and $\Phi(x, \omega) = \sqrt{\pi}t_p(e^2|\mathbf{E}_L|^2/4m\omega_0^2)\exp(i\omega x/c - \omega^2 t_p^2/4)$ is the ponderomotive potential Fourier image. Using expressions (1) and (2) and Maxwell's equations to determine the Fourier image of a low-frequency magnetic field in plasma, we have the equation

$$\frac{\partial^2}{\partial x^2}B_z(x, \omega) - æ^2 B_z(x, \omega)$$
$$= \frac{4\pi\omega}{ce}\frac{\sigma_{yx}(\omega)}{\omega + 4\pi i\sigma_{xx}(\omega)}\frac{\partial^2\Phi(x, \omega)}{\partial x^2}. \quad (3)$$

The notation used here is

$$æ^2 = \frac{1}{c^2}\frac{(\omega^2 - \omega_-^2)(\omega^2 - \omega_+^2)}{\omega_h^2 - \omega^2}, \quad (4)$$

where $\omega_\pm = \sqrt{\omega_L^2 + \Omega^2/4} \pm \Omega/2$ and $\omega_h = \sqrt{\omega_L^2 + \Omega^2}$. The Fourier image of a low-frequency magnetic field in vacuum is described by an equation of the form of (3) in which there is no right-hand side and $æ^2$ is replaced by $-\omega^2/c^2$. Taking into account tangential component continuity of electric and magnetic fields at the plasma boundary, from the joint solution of Eq. (3) and its analog in vacuum, we find the Fourier image of low-frequency magnetic field at the plasma boundary,

$$B_z(0, \omega) = -\frac{\sqrt{\pi}\omega^2}{2(i\omega - æc)^2}\frac{\omega_L^2}{\omega_h^2 - \omega^2}$$
$$\times \frac{\omega_L^2}{\omega_0^2}\frac{I\Omega t_p}{enc^2}\exp\left(-\omega^2 t_p^2/4\right), \quad (5)$$

where $I = c|\mathbf{E}_L|^2/8\pi$ is the laser energy flux density. In formula (5)

$$æ = [\eta(æ^2) - i\eta(-æ^2)\text{sgn}(\omega)]|æ|, \quad (6)$$

where $\eta(x)$ is the Heaviside step function. This form of æ for $æ^2 > 0$ corresponds to a field decrease deep into the plasma, and for $æ^2 < 0$ it corresponds to a wave propagating away from the plasma boundary. The magnetic field strength Fourier image determines the total energy per unit area W, which is radiated into vacuum along the negative direction of the x axis (see Fig. 2), and spectral energy density per unit
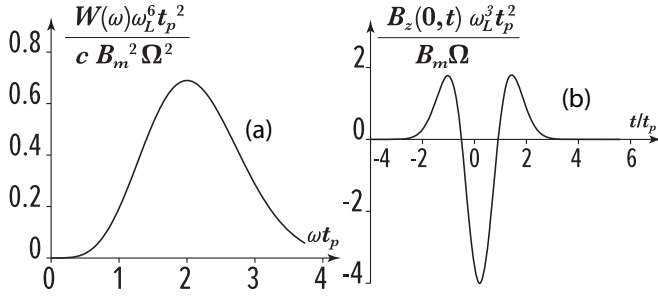
FIG. 2. Plots of (a) the spectral energy density versus frequency and (b) the time dependence of the generated magnetic field at the plasma boundary for a long pulse ($\omega_- t_p \gg 1$).

area $W(\omega)$,

$$
W = \frac{c}{4\pi} \int_{-\infty}^{\infty} dt B_z^2(0,t)
$$
$$
= \frac{c}{4\pi^2} \int_0^{\infty} d\omega |B_z(0,\omega)|^2 = \int_0^{\infty} d\omega W(\omega), \quad (7)
$$

and the generated magnetic field time dependence

$$
B_z(0,t) = \int_{-\infty}^{\infty} \frac{d\omega}{2\pi} B_z(0,\omega) \exp\left(-i\omega t\right). \quad (8)
$$

Dependences of these physical characteristics of the generated pulse on plasma density, constant magnetic field, and laser pulse duration are considered below.

III. STRONG MAGNETIC FIELD

Generation regularities of low-frequency radiation depend on the constant magnetic field magnitude. Let us first consider a strong magnetic field case, in which the electron cyclotron frequency is much larger than the plasma frequency,

$$
\Omega \gg \omega_L. \quad (9)
$$

In this case, for the characteristic frequencies that determine spectral composition features and the shape of the generated radiation pulse, we have the following approximate expressions:

$$
\omega_+ \approx \Omega + \omega_L^2/\Omega > \omega_h \approx \Omega + \omega_L^2/2\Omega \gg \omega_- \approx \omega_L^2/\Omega. \quad (10)
$$

The large difference between the frequencies ω_+ and ω_- allows us to consider three qualitatively different generation modes of low-frequency radiation.

A. Long pulse exposure

If the pulse duration characteristic time t_p satisfies the inequality

$$
\omega_- t_p \approx \omega_L^2 t_p/\Omega \gg 1, \quad (11)
$$

then radiation is mainly generated at frequencies below ω_-. In this case, taking into account Eqs. (4), (5), and (7), for the spectral density and total energy of the low-frequency

radiation we have

$$
W(\omega) = \frac{c}{\pi} B_m^2 \left(\frac{\omega^2 \Omega t_p}{\omega_L^3}\right)^2 \exp\left(-\frac{1}{2}\omega^2 t_p^2\right),
$$
$$
W = \frac{3}{\sqrt{2\pi}} \left(\frac{\Omega}{\omega_L^3 t_p^2}\right)^2 B_m^2 c t_p, \quad (12)
$$

where the notation

$$
B_m = \frac{\omega_L^3}{4\omega_0^2} \frac{I}{enc^2} \quad (13)
$$

is used. In turn, using Eqs. (4) and (5), from (8) we find the magnetic field time dependence

$$
B_z(0,t) = 2B_m \frac{\Omega}{\omega_L^3} \frac{\partial^2}{\partial t^2} \exp\left(-\frac{t^2}{t_p^2}\right). \quad (14)
$$

Note that Eq. (14) is the same as that obtained earlier in [16]. Matching the conditions (9) and (11), in which formulas (12) and (14) are applicable, the plots of the functions $W(\omega)$ and $B_z(0,t)$ are shown in Figs. 2(a) and 2(b). The plots are drawn for $\omega_- t_p = 10$ and $\Omega = 10\omega_L$. In this case, $\omega_L t_p = 100$. In Fig. 2(a) along the vertical axis is the value of the function $c^{-1}W(\omega)(B_m\Omega/\omega_L^3 t_p)^{-2}$, built according to formulas (5) and (7), and the dimensionless frequency ωt_p is plotted along the horizontal axis. According to Fig. 2(a) and formula (12), the dependence of the spectral energy density on frequency is described by a bell-shaped curve with a maximum at $\omega = 2/t_p$. Note that for the selected parameters, the frequency ω_- is equal to $\omega_- \approx 0.01\Omega = 10/t_p$. The time dependence of the generated magnetic field at the plasma boundary, given by formulas (8) and (5), is shown in Fig. 2(b). The vertical axis is the value $B_z(0,t)/(B_m\Omega/\omega_L^3 t_p^2)$, and the horizontal axis is the dimensionless time t/t_p. The curve shape is close to that described by formula (14). The generation of low-frequency radiation mainly occurs during exposure to a laser pulse.

B. Impact of a pulse with intermediate duration

In the strong magnetic field, when inequality (9) is satisfied, with a decrease in the laser pulse duration, conditions are possible when

$$
\omega_- \ll 1/t_p \ll \omega_h \approx \omega_+. \quad (15)
$$

Under these conditions, using formulas (4), (5), and (7), for the spectral energy density of low-frequency radiation, we approximately have

$$
W(\omega) = \frac{c}{\pi} B_m^2 \left(\frac{\omega_L t_p}{\Omega}\right)^2
$$
$$
\times \frac{\omega^4 \exp\left(-\omega^2 t_p^2/2\right)}{[\omega_- \eta(\omega_- - \omega) + (\omega + \sqrt{\omega^2 - \omega_-^2})\eta(\omega - \omega_-)]^4}. \quad (16)
$$

The spectral energy density (16) has a pronounced peak at the frequency ω_-. At frequencies larger than ω_- but less than ω_h, an extraordinary wave propagates deep into the plasma. In the frequency range from ω_- to $\sqrt{2}/t_p$, the function $W(\omega)$ (16) has a wide plateau-like region, and at frequencies larger than $\sqrt{2}/t_p$ this function is exponentially small. A
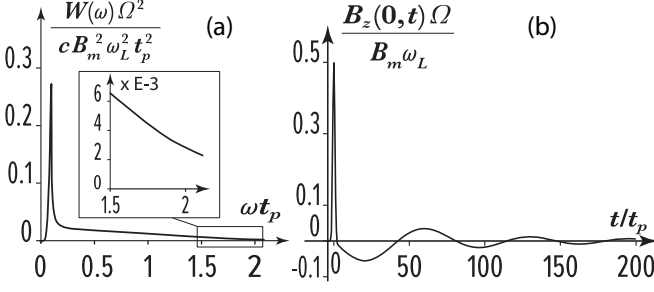
FIG. 3. Plots of (a) the spectral energy density versus frequency and (b) the time dependence of the generated magnetic field at the plasma boundary for intermediate pulse duration ($\omega_- \ll 1/t_p \ll \omega_h$).

FIG. 4. Plots of (a) the spectral energy density versus frequency and (b) the time dependence of the generated magnetic field at the plasma boundary for a short pulse ($\omega_+ t_p \ll 1$).

graph of the function $W(\omega)$, which corresponds to conditions (9) and (15) when formula (16) is applicable, is shown in Fig. 3(a). The graph is plotted for $\omega_- t_p = 0.1$ and $\Omega = 10\omega_L$ for $\omega_L t_p = 1$. The graph clearly shows the features of the function $W(\omega)$ described above. Integrating expression (16) over the frequencies, we find the total energy of the low-frequency radiation,

$$W \approx \frac{c}{5\pi} B_m^2 t_p \left(\frac{\omega_L}{\Omega}\right)^2 \left[\omega_- t_p + \frac{5\sqrt{\pi}}{16\sqrt{2}}\right]. \quad (17)$$

Comparing formulas (12) and (17), we see that the total energy decreases with decreasing pulse duration. The main contribution to W arises from the frequency range that is greater than ω_-, that is, from the plateau-like region of the function $W(\omega)$ (16). The contribution from frequencies less than ω_- gives a small correction proportional to $\omega_- t_p \ll 1$ in the square brackets in formula (17). Note that due to the use of the approximate expression (16), there is no correction $\sim \pi (\Omega/\omega_L)^2 (\Omega t_p) \exp(-\Omega^2 t_p^2/2)$ in the square brackets of formula (17), which is essential at the upper boundary of the applicability region of formula (17) for $\Omega t_p \sim 1$. In turn, taking into account the inequalities (15) and formula (4), after the inverse Fourier transform from (8) and (5) we approximately find the magnetic field dependence versus time,

$$B_z(0, t) = \frac{1}{2} B_m \frac{\omega_L}{\Omega} \left[\exp\left(-\frac{t^2}{t_p^2}\right) - \frac{8\sqrt{\pi} t_p}{\omega_- t} \frac{\partial}{\partial t} J_3(\omega_- t)\right]. \quad (18)$$

The exponential first term in formula (18) arises from integration over frequencies greater than ω_- and describes a relatively large short pulse generated during exposure to a laser pulse. The term containing the Bessel function $J_3(\omega_- t)$ describes oscillations with frequency ω_- decaying with time. The appearance of oscillations is due to the propagation of an extraordinary wave deep into the plasma. For $\omega_- t_p \ll 1$, expression (18) describes with good accuracy the generated magnetic field pulse, which is shown in Fig. 3(b). The curve in Fig. 3(b) is obtained by numerically integrating expression (5) for $\omega_- t_p = 0.1$ and $\Omega = 10\omega_L$. Note that for $\Omega t_p \sim 1$ formula (18) should be written with greater accuracy, like formula (17).
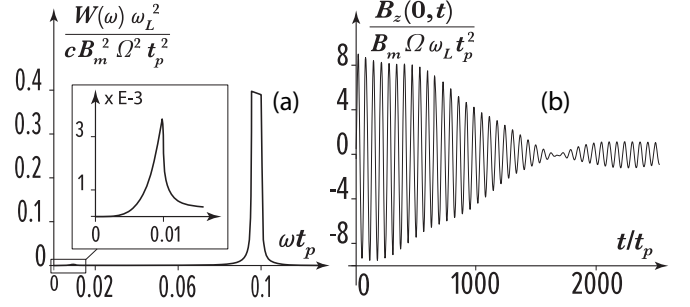
C. Impact of a short pulse

Another regime is realized under the effect of a short laser pulse when its duration satisfies the inequality

$$\omega_+ t_p \ll 1. \quad (19)$$

In this case, the spectral energy density of the radiation can be represented as

$$W(\omega) = \frac{c}{\pi} B_m^2 (\Omega \omega_L t_p)^2 \omega^4 \exp\left(-\frac{\omega^2 t_p^2}{2}\right)$$

$$\times \left\{\frac{\eta(\omega - \omega_+) + \eta[(\omega - \omega_-)(\omega_h - \omega)]}{\left[\omega\sqrt{|\omega^2 - \omega_h^2|} + \sqrt{(\omega^2 - \omega_-^2)|\omega^2 - \omega_+^2|}\right]^4}\right.$$

$$\left. + \frac{\eta(\omega_- - \omega) + \eta[(\omega - \omega_h)(\omega_+ - \omega)]}{\omega_L^4(\omega^2 - \omega_L^2)^2}\right\}. \quad (20)$$

In a strong magnetic field and under the effect of a short laser pulse, the function $W(\omega)$ (20) has a small peak at low frequencies at $\omega = \omega_- \approx \omega_L^2/\Omega$ and a large peak at high frequencies at $\omega = \omega_h \approx \Omega + \omega_L^2/2\Omega$. In a relatively narrow frequency range from ω_h to ω_+, the function $W(\omega)$ decreases slightly, remaining very large. A sharp decrease in $W(\omega)$ starts at $\omega > \omega_+ \approx \Omega + \omega_L^2/\Omega$. This spectral energy density behavior is clearly illustrated in Fig. 4(a). The curve in Fig. 4(a) is plotted for $\omega_+ t_p = 0.1$ and $\omega_-/\omega_+ = 0.1$, which corresponds to $\omega_L/\Omega \approx 0.35$. The peak value of the function $W(\omega)$ at $\omega = \omega_h$ exceeds ones at $\omega = \omega_-$ by about $(\Omega/\omega_L)^4 \approx 65$ times. Integrating expression (20) over the frequencies, we find the total energy of the low-frequency radiation, which is mainly determined by the contribution from high frequencies,

$$W \approx \frac{2c}{3\pi} B_m^2 \Omega t_p^2. \quad (21)$$

In accordance with the above-described behavior of the spectral energy density, the generated magnetic field time dependence (8) is mainly determined by the contribution from the high-frequency region. In Fig. 4(b), a graph of the function $B_z(0, t)$ obtained for $\omega_+ t_p = 0.1$ and $\omega_- \omega_+ = 0.1$ is shown. According to Fig. 4(b), the generated magnetic field pulse contains fast oscillations at the frequency ω_h, and its envelope changes with the beat frequency $\omega_+ - \omega_h$.
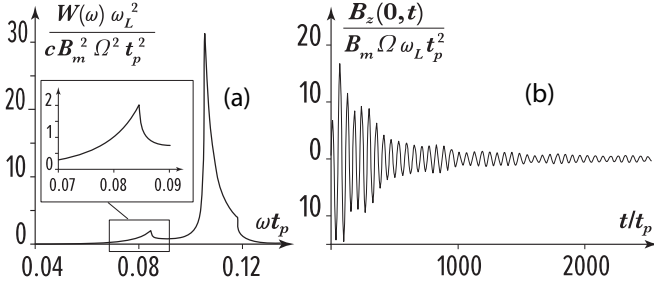
FIG. 5. Plots of (a) the spectral energy density versus frequency and (b) the time dependence of the generated magnetic field at the plasma boundary for a short pulse ($\omega_L t_p \ll 1$) and weak magnetic field.

IV. WEAK MAGNETIC FIELD

In a weak magnetic field, the electron cyclotron frequency is much lower than the plasma frequency

$$\Omega \ll \omega_L. \qquad (22)$$

Herein, the frequencies $\omega_\pm$ and ω_h are close to ω_L:

$$\omega_\pm \approx \omega_L(1 \pm \Omega/2\omega_L),$$
$$\omega_h \approx \omega_L\left(1 + \Omega^2/2\omega_L^2\right). \qquad (23)$$

Under these conditions, two different modes of low-frequency radiation generation are possible.

A. Impact of a long pulse

When the inequality

$$\omega_L t_p \gg 1 \qquad (24)$$

holds, the radiation generation mainly occurs at frequencies less than ω_L. For such large t_p the magnetic field dependence versus time, spectral energy density, and total energy are described by expressions (14) and (12) [see also Figs. 1(b) and 1(a)]. Note that for $\omega_L t_p \sim 1$, expression (12) should be clarified by adding the correction $\sim B_m^2 c t_p (\omega_L/\Omega)^2 \exp(-\omega_L^2 t_p^2/2)$, which is essential for $\omega_L \gg \Omega$. The same addition is required for formula (14).

B. Impact of a short pulse

When exposed to a short laser pulse,

$$\omega_L t_p \ll 1. \qquad (25)$$

In this case, the spectral energy density dependence versus frequency is described by formula (20) and is shown in Fig. 5(a), plotted for $\omega_L/\Omega = 3$, $\omega_L t_p = 0.1$. According to Fig. 5(a), $W(\omega)$ has a sharp peak at $\omega_h \approx \omega_L \approx 0.105/t_p$. The second peak occurs at a lower frequency, $\omega_- \approx 0.085/t_p$. In accordance with formula (20) its height is $(\omega_L/\Omega)^2 = 9$ times less than the height of the main peak at the frequency ω_h. Unlike Fig. 4(a), where in the frequency range $\omega_h < \omega < \omega_+$ the spectral energy density decreased slightly and a sharp decrease began after the frequency ω_+, in Fig. 5(a) a sharp decrease in $W(\omega)$ occurs in the region $\omega_h < \omega < \omega_+$. When the frequency exceeds $\omega_+ \approx 0.118/t_p$, the $W(\omega)$ function decreases even more. For a total radiation energy in accordance
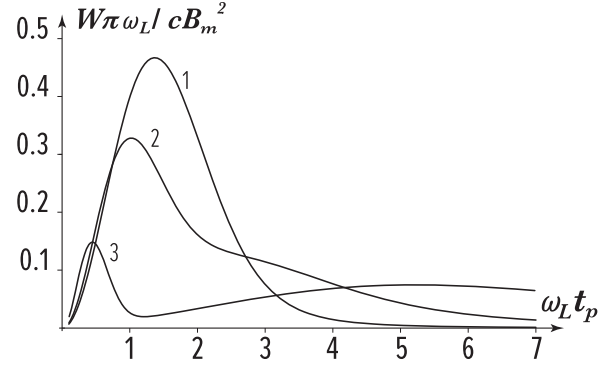
with formula (20) we get the expression

$$W \approx \frac{2c}{3\pi} B_m^2 \omega_L t_p^2. \qquad (26)$$

The main contribution to W (26) comes from the frequency range $\omega_- < \omega < \omega_+$. The generated magnetic field time dependence (8) in this case is determined by the presence of the sharp peak at the frequency ω_h and is shown in Fig. 5(b). According to Fig. 5(b), the generated magnetic field contains fast oscillations with a period of $60t_p$, which correspond to the frequency ω_h. These fast oscillations have an envelope that has oscillations with a period of $\approx 500 t_p$, which corresponds to a beat with a frequency of $\omega_+ - \omega_h \approx 0.013/t_p$. Due to a strong decrease in the spectral energy density in the region $\omega_h < \omega < \omega_+$ beats in Fig. 5(b) are less pronounced than in Fig. 4(b). The oscillations of the generated field in Fig. 3(b) [see also (18)], Fig. 4(b), and Fig. 5(b) are conditioned by the possibility of plasma oscillations at the corresponding frequencies. According to Fig. 3(b) and (18) in strong magnetic field, oscillations occur at the frequency ω_-. Also in strong magnetic field but under the effect of a short laser pulse, the oscillation frequency is close to $\omega_h \sim \Omega$ [see Fig. 4(b)]. In a weak magnetic field, when $\omega_h \sim \omega_L$, the oscillation frequency is close to the plasma one. As for other low-frequency radiation generation mechanisms (see, for example, [17–19]), oscillations at the frequency ω_L are most pronounced when exposed to a short laser pulse when $\omega_L t_p \ll 1$.

V. CONCLUSION

Let us discuss in more detail the dependence of the total low-frequency radiation energy W on the electron cyclotron frequency Ω and the time t_p, which determines the laser pulse duration. We assume that the electron plasma frequency is fixed, which corresponds to the consideration of a plasma with constant density. Graphs of the function $W\pi\omega_L/cB_m^2$ versus $\omega_L t_p$ for several values of the ratio Ω/ω_L are shown in Fig. 6. In a weak magnetic field, when $\Omega = 0.3\omega_L$, the W function has a maximum at $\omega_L t_p \approx 1.3$. At the maximum $W \approx 0.47cB_m^2/\pi\omega_L$. At the same time, in accordance with Fig. 5(a), generation occurs mainly at frequencies close to the electron plasma frequency $\omega \sim 1/t_p \sim \omega_L$. In a stronger magnetic field, when $\Omega = \omega_L$, the maximum of the W function is

FIG. 6. Plot of the total low-frequency radiation energy W versus $\omega_L t_p$ for several values of the ratio Ω/ω_L: (1) $\Omega = 0.3\omega_L$, (2) $\Omega = \omega_L$, and (3) $\Omega = 3\omega_L$.

reached at a slightly shorter pulse duration, when $\omega_L t_p \approx 1$, and its value decreases: $W \approx 0.33 c B_m^2/\pi \omega_L$. In this case, the generation band is somewhat wider, and the generation maximum still falls at the frequencies $\omega \sim 1/t_p \sim \omega_L$. At an even higher electron cyclotron frequency, when $\Omega = 3\omega_L$, the W function has two maxima [see Fig. 4(a)]. The first maximum is reached at $\omega_L t_p \approx 0.5$, when $W \approx 0.15 c B_m^2/\pi \omega_L$. In this case, $\Omega t_p \approx 1.5$, and in accordance with Fig. 4(a), generation occurs mainly at frequencies comparable to the cyclotron frequency. The second maximum $W \approx 0.07 c B_m^2/\pi \omega_L$ occurs at a longer pulse duration, when $\omega_L t_p \approx 5$. In this case $\omega_L^2 t_p/\Omega \approx 1.6$, and according to Fig. 3(a), the low-frequency radiation spectrum has a peak at the frequency $\sim \omega_-$ and a relatively wide band in the frequency range below $1/t_p$. It follows from the above discussion of the W function's behavior that the most efficient generation occurs at $t_p \sim 1/\omega_L$ and at cyclotron frequencies lower than the electron plasma frequency. However, the cyclotron frequency of electrons must be much higher than the effective collision frequency. Herein radiation is generated mainly at frequencies comparable to the plasma frequency. The generation frequency can be increased in a strong magnetic field when cyclotron frequency exceeds plasma frequency and generation occurs at frequencies $\sim \Omega$. However, the generation efficiency decreases in strong magnetic fields (see Fig. 6). In conclusion, we presented an estimate of the low-frequency radiation energy per unit area under optimal conditions. Let us assume that plasma with the electron density of $n = 10^{17}$ cm^{-3} interacts with a laser pulse with a frequency of $\omega_0 = 1.8 \times 10^{15} s^{-1}$, a pulse duration of 120 fs, and energy flux density $I = 10^{15}$ W/cm^2. Under these conditions $t_p \approx 70$ fs, $\omega_L \approx 1.8 \times 10^{13}$ s^{-1}, and $\omega_L t_p \approx 1.3$, and the effective frequency of electron collisions is much lower than the plasma frequency. We consider the cyclotron frequency of electrons to be lower than the plasma frequency, which occurs when the constant magnetic field strength is less than 1 MG. Here, in accordance with Fig. 6 and formula (13), we have $B_m \approx 100$ G and $W \approx 3$ μJ/cm^2. In this case, the generation maximum occurs at a frequency close to the plasma one, $\omega \approx \omega_L \approx 1.8 \times 10^{13}$ s^{-1}, or ≈ 3 THz.

[1] J. Yoshii, C. H. Lai, T. Katsouleas, C. Joshi, and W. B. Mori, Phys. Rev. Lett. **79**, 4194 (1997).

[2] N. Spence, T. Katsouleas, P. Muggli, W. B. Mori, and R. Hemker, Phys. Plasmas **8**, 4995 (2001).

[3] M. I. Bakunov, S. B. Bodrov, A. V. Maslov, and A. M. Sergeev, Phys. Rev. E **70**, 016401 (2004).

[4] L. M. Gorbunov and A. A. Frolov, Plasma Phys. Rep. **32**, 500 (2006).

[5] A. K. Malik, K. P. Singh, and V. Sajal, Phys. Plasmas **21**, 073104 (2014).

[6] R. K. Singh and R. P. Sharma, Phys. Plasmas **21**, 113109 (2014).

[7] D. Singh and H. K. Malik, Plasma Sources Sci. Technol. **24**, 045001 (2015).

[8] F. Bakhtiari, M. Esmaeilzadeh, and B. Ghafary, Phys. Plasmas **24**, 073112 (2017).

[9] R. K. Singh, M. Singh, S. K. Rajouria, and R. P. Sharma, Phys. Plasmas **24**, 073114 (2017).

[10] A. K. Malik, H. K. Malik, and U. Stroth, Phys. Rev. E **85**, 016401 (2012).

[11] A. K. Malik and K. P. Singh, Laser Part. Beams **33**, 519 (2015).

[12] P. Varshney, V. Sajal, A. Upadhyay, J. A. Chakera, and R. Kumar, Laser Part. Beams **35**, 279 (2017).

[13] M. Abedi-Varaki and S. Jafari, J. Opt. Soc. Am. B **35**, 1165 (2018).

[14] K. N. Ovchinnikov and S. A. Uryupin, J. Russ. Laser Res. **40**, 467 (2019).

[15] V. E. Grishkov, K. N. Ovchinnikov, and S. A. Uryupin, J. Russ. Laser Res. **42**, 538 (2021).

[16] K. N. Ovchinnikov and S. A. Uryupin, Phys. Rev. E **103**, 033205 (2021).

[17] D. K. Kalluri, IEEE Trans. Plasma Sci. **16**, 11 (1988).

[18] V. A. Kostin and N. V. Vvedenskii, New J. Phys. **17**, 033029 (2015).

[19] V. E. Grishkov and S. A. Uryupin, J. Appl. Phys. **128**, 203102 (2020).